Eur. Phys. J. D **16**, 387–390 (2001)

THE EUROPEAN PHYSICAL JOURNAL D

EDP Sciences

Far-infrared response of quantum-dot molecules

M. Valín-Rodríguez, A. Puente, and Ll. Serra[a]

Departament de Física, Universitat de les Illes Balears, E-07071 Palma de Mallorca, Spain

Received 29 November 2000

Abstract. We report an analysis of the dipole response of a symmetric quantum-dot molecule as a function of the dot-dot separation and intensity of a perpendicular magnetic field. The potential barrier is assumed proportional to the interdot distance using a two-center oscillator potential. The results are obtained within the symmetry-unrestricted TDLSDA. It is shown that the FIR details, specially the fragmentation of the low-energy brach, are quite sensitive to the interdot separation and that in both the small and large separation limits the results converge towards the analytic Kohn's magnetoplasmon energies. The validity of the LSDA is checked by comparison with the Hartree-Fock dipole spectrum in one case.

PACS. 73.20.-r Electron states at surfaces and interfaces – 78.20.Bh Theory, models and numerical simulation

1 Introduction

Nanolithography and etching techniques have nowadays developed to the point that they can be used to fabricate an important variety of quantum dots (QD) and general electronic nanostructures [1]. This has obviously, given a strong impetus to the experimental research in nanostructures, motivating an intense theoretical activity as well. Much effort has been devoted to the understanding of isolated quantum dots (see for instance Ref. [2]) but, in practice, these systems are usually produced in more or less regular arrays with characteristic dot-dot separations. The large separation limit is normally considered, although the relevance of inter-dot interactions is something that must be taken into account. Indeed, this point has been addressed by Bakshii *et al.* [3] and by van Zyl *et al.* [4] who concluded that in the experiments by Demel *et al.* [5] interdot coupling is very weak.

Interdot interactions are most important in quantum-dot molecules (QDM), which are composed of two (close) quantum dots. These systems have motivated a strong theoretical interest [6,7], much like that drawn by quantum-dot (artificial) atoms, attributed in part to their potential impact on nanoelectronics technology. In this paper we report on a calculation of the far-infrared (FIR) dipole response in QDM's, analyzing the dependence on both the dot-dot separation and the magnetic field. In the limits of vanishing and large dot-dot separation the FIR spectrum is well explained by Kohn's theorem which yields the dipole frequencies for a purely parabolic, isolated, dot as $\omega_{\pm} = \sqrt{\omega_0^2 + \omega_c^2/4} \pm \omega_c/2$, where ω_0 is the parabola coefficient and $\omega_c = eB/mc$ the cyclotron frequency. However, for intermediate separations the dipole response strongly deviates from the prediction of Kohn's theorem exhibiting a richer structure. This fragmentation must be attributed to the increasing importance of Landau damping in the molecular electronic distributions, manifested by a larger density of particle-hole transitions at the energy of the collective excitations. Large magnetic fields contribute also to increase the fragmentation since they favour an increase of the electronic density in the interdot region and therefore, effectively reduce the dot-dot separation.

The rest of the paper is organized as follows. The model used to describe the ground state and time-dependent oscillations of the QDM's is presented in Sec. 2. Section 3 is devoted to the results and finally, the conclusions are drawn in Sec. 4.

2 The model

2.1 Ground state

We describe QDM's using the model proposed by Yannouleas and Landman [6], which was inspired by analogous two-center oscillator potentials developed in nuclear [8] and cluster physics [9]. The external potential felt by the electrons is purely parabolic in the x-direction and is a piecewise function in the y-direction. The reader is addressed to Ref. [6] for details and we only mention here that the *free parameters* of the potential are the parabola coefficient ω_0 (the same for x and y-directions as well as for the two centers), the centers separation Δ and the interdot barrier height V_b. The results that will be presented below correspond to a QDM containing 12 electrons with parabola coefficient $\omega_0 = 0.5H^*$ [10] and varying separation and barrier height. A proportionality between barrier height and separation is assumed. In order to reproduce

[a] e-mail: DFSLSC4@clust.uib.es

a smoothly increasing barrier for small separations we assume first a linear increase $V_b(\Delta) = \Delta/8$ (in atomic units) for $\Delta < \Delta_1$, and eventually join it with a quadratic $V_b(\Delta) = \Delta^2/85.1 - 0.77$, for $\Delta > \Delta_1$. The transition point is chosen as $\Delta_1 = 15$, which determines the precise numerical values. In fact, we will report results for the three cases $(\Delta, V_b) = (3, 0.375)$, $(15, 1.875)$ and $(24, 6)$, which are taken as representative examples of small, intermediate and large separation, respectively. As we will show below, the three chosen QDM's have quite different electronic distributions, ranging from a compact structure to the situation of two independent dots.

The electronic structure has been described within the local-spin-density approximation (LSDA) by solving the Kohn-Sham equations for the single-particle orbitals,

$$\left[\frac{1}{2m} \left(-i\hbar\nabla + \frac{e}{c}\mathbf{A}(\mathbf{r}) \right)^2 + V_\eta(\mathbf{r}) + g^* \mu_B B s_z \right] \varphi_{i\eta}(\mathbf{r}) = \epsilon_{i\eta} \varphi_{i\eta}(\mathbf{r}), \quad (1)$$

where $\eta = \uparrow, \downarrow$ labels the two spin components and $\mathbf{A}(\mathbf{r}) \equiv B/2(-y, x)$ is the vector potential in the symmetric gauge for the magnetic field $\mathbf{B} = B\hat{\mathbf{z}}$. The last piece within the brackets is the Zeeman term depending on the spin s_z, the Bohr magneton μ_B and the effective gyromagnetic factor g^* (for bulk GaAs $g^* = -0.44$). No symmetry is imposed to the orbitals $\varphi_{i\eta}(\mathbf{r})$ which are numerically obtained in coordinate space by discretizing the equations in a uniform grid of points. This symmetry unrestricted method was developed in Ref. [11] to study deformed quantum dots. The reader is addressed to this reference for technical details of the numerical approach as well as for the ingredients of the energy functional giving $V_\eta(\mathbf{r})$ and the integration technique.

A well known drawback of LSDA when describing molecules is its trend to smear the electronic density even by delocalizing the orbitals [12]. For instance, with an odd total electron number the large separation limit of a symmetric QDM would correspond within LSDA to both dots having a half-integer electron number, which is an obviously unphysical result. In order to avoid this deficiency, we have only considered the $N = 12$ QDM, which splits into two equal 6-electron dots. In this way both the zero- and large-separation limits correspond to closed-shell systems that can be properly considered within LSDA. Furthermore, we have also performed Hartree-Fock calculations, which can describe in a more realistic way the electronic localization in QDM's [6], in some cases, with the purpose to provide additional support to the LSDA results. This point is further discussed in Sec. 3.

2.2 Time-dependent oscillations

The FIR absorption will be obtained from the time dependent dipole signal

$$D(t) = \mathbf{e} \cdot \left\langle \sum_{i=1}^{N} \mathbf{r}_i \right\rangle, \quad (2)$$

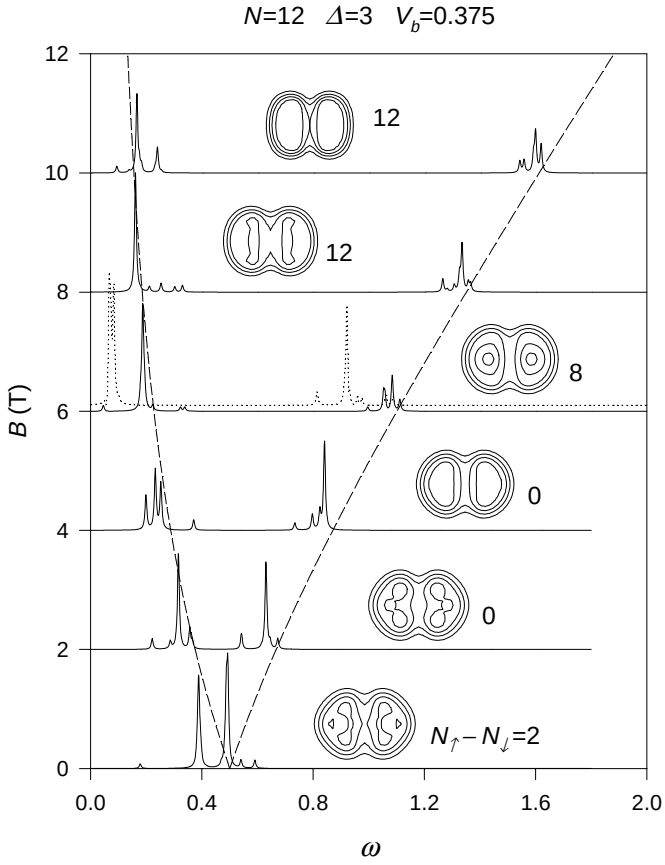

Fig. 1. FIR absorption spectrum for the 12-electron QDM mentioned in Sec. 2, for the small separation and interdot barrier. Each spectrum is plotted in arbitrary but linear scale and its corresponding magnetic field is indicated by the vertical axis. The horizontal axis give energies in effective atomic units. The dashed lines show the dispersion of the analytical Kohn energies (Sec. 1) and the dotted curve (for $B = 6$ T) shows the independent particle-hole transitions. At each magnetic field the density contour lines and total polarization is also given.

where $\mathbf{e}$ is the polarization direction. This real-time technique is a powerful method which does not require any symmetry constraint and therefore, it is quite appropriate to address the oscillations in QDM's. We have applied it in Refs. [11,13] to study charge and current modes in elliptical quantum dots. In practice, the time-dependent Kohn-Sham equations,

$$i\,\hbar \frac{\partial}{\partial t}\varphi_{i\eta}(\mathbf{r}, t) = \left[\frac{1}{2m} \left(-i\hbar\nabla + \frac{e}{c}\mathbf{A}(\mathbf{r}) \right)^2 + V_\eta(\mathbf{r}) + g^* \mu_B B s_z \right] \varphi_{i\eta}(\mathbf{r}, t), \quad (3)$$

or the analogous Hartree-Fock ones, allow one to monitor $D(t)$ following an initial rigid dipole shift in the $\mathbf{e}$ direction, being the corresponding absorption cross section given by the Fourier transform [11]

$$\sigma(\omega) \approx \frac{\omega}{2\pi} \left| \int dt\, D(t)\, \exp(i\omega t) \right|. \quad (4)$$

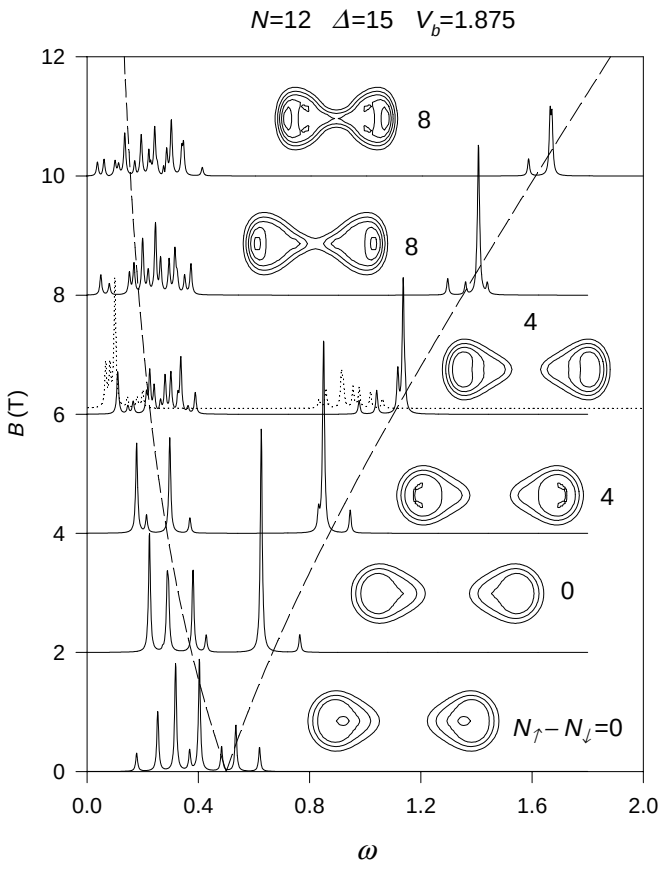

Fig. 2. Same as Fig. 1 for the intermediate dot-dot separation and barrier height.

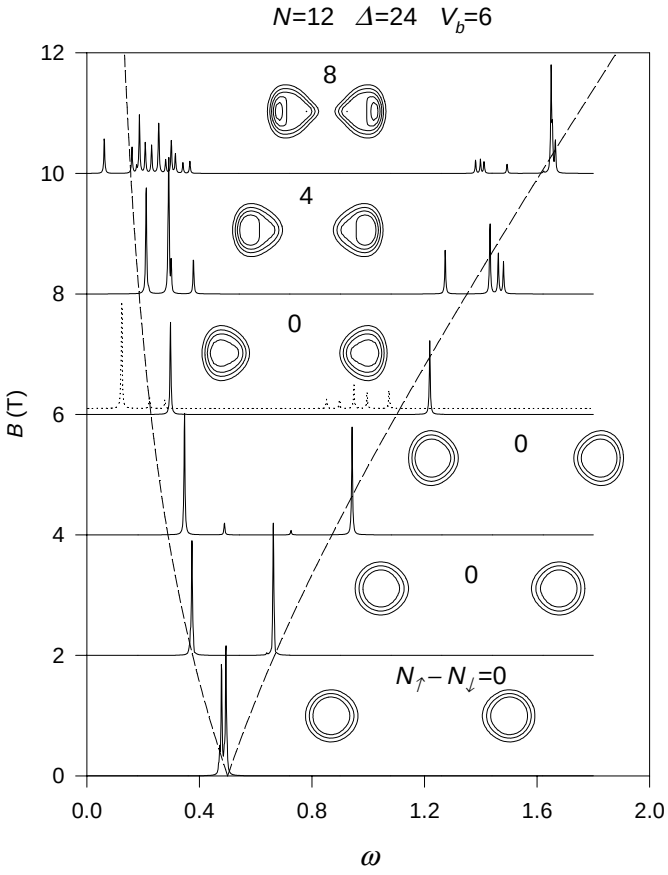

Fig. 3. Same as Fig. 1 for the large dot-dot separation and barrier height.

3 Results

Figures 1-3 contain the main results of the paper. They show the dipole spectra for the three separations mentioned in Sec. 2.1, as a function of the applied magnetic field. The spectra are drawn in linear scale but with arbitrary units and the vertical axis indicates, at the intersection with each baseline, the corresponding magnetic field. Also shown in the Figs. are the contour lines of the total density, for the different magnetic fields.

The first case (Fig. 1) corresponds to two overlapping dots and therefore to the situation of a strong dot-dot influence. We notice that the $B = 0$ spectrum has two dominant peaks, reflecting the splitting due to the elliptical electronic distribution. When B increases the strength separates into two clear branches, with some fragmentation, that on average follow Kohn's analytical formula given by the dashed line (Sec. 1). Figure 2 corresponds to the intermediate separation and barrier height. The dot-dot interaction is still very important as one realizes from the density contour lines. We notice that the fragmentation of the FIR spectrum is dramatically increased with respect to that of Fig. 1, specially for the low energy branch. This fragmentation is due to a more important role of the Landau damping mechanism. To prove this we show as a dotted line the independent particle-hole transitions at $B = 6$ T. For clarity the spectrum has been slightly shifted in the vertical direction. It is clear that the number of particle-hole transitions in Fig. 2 is higher than in Fig. 1, and they are also closer in energy to the peaks of the interacting response, which favours the damping of the collective motion. It is worth to mention that a similar mechanism was shown by Yannouleas to be the source of an important fragmentation in the absorption of potassium clusters [14].

Figure 3 shows the results for the well separated dots. As one would expect, in this case the FIR absorption at low B's has a much cleaner structure, with practically no fragmentation in either branch for $B \leq 6$ T. In this regime each dot is essentially decoupled from the other one and indeed, we have checked that the spectrum of a single dot coincides with the result for the molecule. We notice however that the peaks slightly deviate from Kohn's prediction for $B = 4$ and 6 T due to the deviation from a perfect parabola introduced by the inter-dot barrier. Our barrier parameterization thus allows the possibility of having independent but non-parabolic dots in the QDM. A qualitatively different spectrum appears for $B \geq 8$ T, with a fragmentation similar that of Fig. 2. The reason for this becomes obvious when looking at the density contours for these magnetic fields. At large B's the electronic density is deformed by pulling electrons towards the inter-dot region and therefore in an effective way the interdot

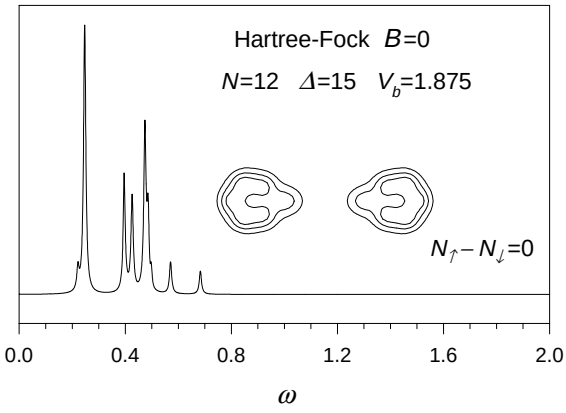

Fig. 4. Same as lower panel of Fig. 2 but within Hartree-Fock theory.

distance is reduced thus increasing the dot-dot coupling. The effective dot-dot attraction at large magnetic fields is also quite evident from Fig. 2. It can be hinted from the general property that large magnetic fields induce smaller electronic orbits and therefore, more compact QDM's.

The net magnetization $2S \equiv N_\uparrow - N_\downarrow$ is also indicated in Figs. 1-3. Obviously, when increasing the magnetic field the molecule tends to spin polarize. However, the spin gain with B is faster for the small separation (Fig. 1) than for the intermediate and large distances (Figs. 2, 3). Quite interestingly, we also notice that for the small separation the QDM has a non-vanishing spin ($2S = 2$) even at $B = 0$. We remark that the isolated parabolic dots with $N = 12$ and 6 electrons are closed shell systems with $S = 0$. Therefore, our results indicate that when the two dots begin to separate in the QDM the spin increases, reaching a maximum for some distance and eventually decreases again to the $S = 0$ limit for large dot-dot distances. This mechanism of spin gain at $B = 0$ by deformation of closed shell systems has also been obtained in the quantum dot calculations of Refs. [15,16].

Finally, Fig. 4 shows the result for the intermediate separation at $B = 0$ obtained within Hartree-Fock theory. In this case each single-particle wave function is completely localized in one or the other dot; contrarily to the Kohn-Sham results for which some orbitals are shared by the two dot centers. Nevertheless, the agreement with the lower panel of Fig. 2 is rather good, both in the spectrum fragmentation and in the shape of the density contours. This supports the use of the TDLSDA and indicates, in our opinion, that the Kohn-Sham orbitals are a *mathematical* ingredient of density-functional theory that, as opposed to electron spin densities, lack a fundamental importance. A more detailed presentation of the Hartree-Fock results will be given elsewhere.

4 Conclusions

The FIR absorption of three representative QDM's has been obtained within the time-dependent LSDA as a function of the applied magnetic field. The three cases correspond to a QDM with 12 electrons with a short, intermediate and large dot-dot separation, respectively. The inter-dot barrier has been parameterized in order to model the transition from a compact structure to two independent 6-electron dots. Both for vanishing and very large separations the spectrum can be understood in terms of Kohn's theorem. For intermediate separations however it shows a sizeable fragmentation which is more important for the low energy brach. This fragmentation is a manifestation of the Landau damping and it first increases with separation, reaching a maximum for a certain distance, and then decreases to reach the pure magnetoplasmon (Kohn) modes again. Large magnetic fields tend to couple the two dots by introducing an effective attraction and also favour the spectrum fragmentation. The dependence of the ground state spin and density distributions with magnetic field for the different QDM's has been discussed.

This work has been performed under Grant No. PB98-0124 from DGESeIC, Spain.

References

1. D. Bimberg, M. Grundmann, N.N. Ledentsov, *Quantum dot heterostructures* (Wiley, Chichester, 1999).
2. L. Jacak, P. Hawrylak, A. Wójs, *Quantum dots* (Springer, Berlin, 1998).
3. P. Bakshi, D.A. Broido, K. Kempa, Phys. Rev. B **42**, 7416 (1990).
4. B.P. van Zyl, E. Zaremba, D.A.W. Hutchinson, Phys. Rev. B **61**, 2107 (2000).
5. T. Demel, D. Heitmann, P. Grambow, K. Ploog, Phys. Rev. Lett. **64**, 788 (1990).
6. C. Yannouleas, U. Landmann, Phys. Rev. Lett. **82**, 5325 (1999).
7. R.N. Barnet *et al.*, Eur. Phys. J. D **9**, 95 (1999).
8. J. Maruhn, W. Greiner, Z. Phys. **251**, 431 (1972).
9. C. Yannouleas, U. Landman, J. Phys. Chem. **99**, 14577 (1995).
10. We use effective atomic units $H^* = (m/m_e\kappa^2)H$, $a_B^* = (m_e/m)\kappa\, a_B$, given in terms of the electron effective mass $m = m^* m_e$, the material dielectric constant κ and the usual Hartree unit ($H = 27.21$ eV) and Bohr radius ($a_B = 0.529$ Å). Taking the GaAs values $\epsilon = 12.4$ and $m^* = 0.067$ we get $H^* \approx 12$ meV and $a_0^* \approx 98$ Å.
11. A. Puente, Ll. Serra, Phys. Rev. Lett. **83**, 3266 (1999).
12. *Recent developments and applications of modern density functional theory*, edited by J.M. Seminario (Elsevier, Amsterdam, 1996).
13. Ll. Serra, A. Puente, E. Lipparini, Phys. Rev. B **60**, R13966 (1999).
14. C. Yannouleas, Chem. Phys. Lett. **193**, 587 (1992).
15. K. Hirose, N.S. Wingreen, Phys. Rev. B **59**, 4604 (1999).
16. D.G. Austing *et al.*, Phys. Rev. B **60**, 11514 (1999).